Topology Preserving 3D Thinning Algorithms Using Four and Eight Subfields

Gábor Németh, Péter Kardos, and Kálmán Palágyi

Department of Image Processing and Computer Graphics,
University of Szeged, Hungary
{gnemeth,pkardos,palagyi}@inf.u-szeged.hu

Abstract. Thinning is a frequently applied technique for extracting skeleton-like shape features (i.e., centerline, medial surface, and topological kernel) from volumetric binary images. Subfield-based thinning algorithms partition the image into some subsets which are alternatively activated, and some points in the active subfield are deleted. This paper presents a set of new 3D parallel subfield-based thinning algorithms that use four and eight subfields. The three major contributions of this paper are: 1) The deletion rules of the presented algorithms are derived from some sufficient conditions for topology preservation. 2) A novel thinning scheme is proposed that uses iteration-level endpoint checking. 3) Various characterizations of endpoints yield different algorithms.

Keywords: 3D image analysis, Shape representation, Feature extraction, Thinning algorithms, Topology preservation.

1 Introduction

Skeleton-like shape features (i.e., centerline, medial surface, and topological kernel [1]) extracted from volumetric binary images play an important role in numerous applications of image processing, pattern recognition, and visualization, such as topological analysis [2], measurement [12], surface generation [4], shape matching [15], or automatic navigation [16].

Parallel thinning algorithms [3] are capable of extracting skeleton-like shape descriptors in a topology preserving way [5]. They use parallel reduction operations: some points having value of "1" in a binary image that satisfy certain topological and geometric constraints are deleted (i.e., changed some "1" points to "0" ones) simultaneously, and an iteration step is repeated until stability is achieved. Thinning algorithms use operators that delete some points which are not endpoints, since preserving endpoints provides important geometrical information relative to the shape of the objects.

Thinning has a major advantage over other skeletonization methods: it is capable of extracting all the three kinds of skeleton-like shape features: surface-thinning algorithms extract *medial surface*s by preserving *surface-endpoint*s, curve-thinning algorithms produce *centerline*s by preserving *curve-endpoint*s,

A. Campilho and M. Kamel (Eds.): ICIAR 2010, Part I, LNCS 6111, pp. 316–325, 2010.

and *topological kernels* (i.e., minimal structures which are topologically equivalent to the original objects) can be generated if no endpoint criteria are considered during the thinning process. Medial surfaces are generally extracted from general shapes, tubular structures can be represented by their centerlines, and topological kernels are fairly useful in topological description. Note that thinning is sensitive to coarse object boundaries, hence it is to be coupled with an efficient pruning method [14].

One type of parallel thinning algorithms is the *subfield-based* technique [3]. In existing subfield-based 3D thinning algorithms, the digital space denoted by $\mathbb{Z}^3$ is partitioned into two [7,8,11], four [9], and eight [1] subfields which are alternatively activated (see Fig. 1b-d). At a given iteration step of a k-subfield algorithm, k successive parallel reductions associated to the k subfields are performed. In each parallel reduction, some border points in the active subfield can be designated to be deleted.

In [11], we proposed some 2-subfield 3D thinning algorithms that are based on Ma's sufficient conditions for parallel reduction operators [6]. In this paper, we introduce a set of 4- and 8-subfield 3D thinning algorithms that satisfy some sufficient criteria for such operators. In addition, a new thinning scheme with iteration-level endpoint checking is suggested.

2 Basic Notions and Results

Let p be a point in the 3D digital space $\mathbb{Z}^3$. Let us denote $N_j(p)$ (for $j = 6, 18, 26$) the set of points that are j-*adjacent* to point p (see Fig. 1a).

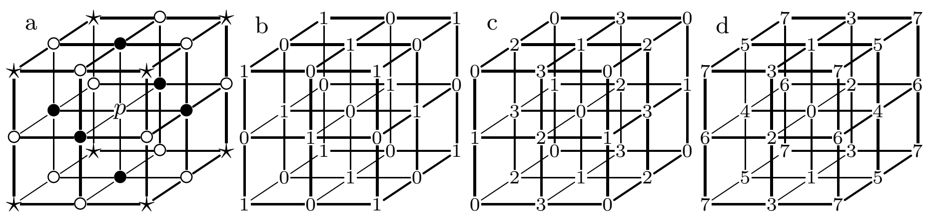

Fig. 1. Frequently used adjacencies in $\mathbb{Z}^3$ (a). The set $N_6(p)$ contains point p and the 6 points marked "•". The set $N_{18}(p)$ contains $N_6(p)$ and the 12 points marked "○". The set $N_{26}(p)$ contains $N_{18}(p)$ and the 8 points marked "⋆".
The divisions of $\mathbb{Z}^3$ into 2 (b), 4 (c), and 8 (d) subfields. If partitioning into k subfields is considered, then points marked "i" are in the subfield $SF_k(i)$ ($k = 2, 4, 8,\ i = 0, 1, \ldots, k-1$).

The *3D binary* (26, 6) *digital picture* $\mathcal{P}$ is a quadruple $\mathcal{P} = (\mathbb{Z}^3, 26, 6, B)$ [5], where each element of $\mathbb{Z}^3$ is called a *point* of $\mathcal{P}$, each point in $B \subseteq \mathbb{Z}^3$ has a value of "1", each point in $\mathbb{Z}^3 \backslash B$ has a value of "0". 26-connectivity (i.e., the reflexive and transitive closure of the 26-adjacency relation) is considered for "1" points forming the objects, and 6-connectivity (i.e., the reflexive and transitive closure of the 6-adjacency) is considered for "0" points [5] (see Fig. 1a).

A "1" point is called a *border point* in a $(26, 6)$ picture if it is 6-adjacent to at least one "0" point. A "1" point is called an *interior point* if it is not a border point.

A *parallel reduction operator* changes a set of "1" points to "0" ones (which is referred to as deletion). A 3D parallel reduction operator does *not* preserve topology if any object (i.e., maximal 26-connected component of "1" points) is split or is completely deleted, any cavity (i.e., maximal 6-connected component of "0" points) is merged with another cavity, a new cavity is created, or a hole (that donuts have) is eliminated or created.

A "1" point is called a *simple* point if its deletion does not alter the topology of the image [5]. Note that simplicity of point p in $(26, 6)$ images is a local property that can be decided by investigating the set $N_{26}(p)$ [5].

Parallel reduction operators delete a set of "1" points. Hence we need to consider what is meant by topology preservation when a number of "1" points are deleted simultaneously. First we define the concept of simple sets.

Definition 1. [6] *The set of "1" points* $D = \{d_1, \ldots, d_k\} \subset B$ *in a picture* $\mathcal{P} = (\mathbb{Z}^3, 26, 6, B)$ *is called a* simple set *if* D *can be arranged in a sequence* $\langle d_{i_1}, \ldots, d_{i_k} \rangle$ *in which point* d_{i_1} *is simple in* $\mathcal{P}$*, and each point* d_{i_j} *is simple in* $(\mathbb{Z}^3, 26, 6, B \setminus \{d_{i_1}, \ldots, d_{i_{j-1}}\})$*, for* $j = 2, \ldots, k$*. (By definition, let the empty set be simple.)*

The following theorem provides *sufficient conditions* for 3D parallel reduction operators to preserve topology.

Theorem 1. [6] *A 3D parallel reduction operation* preserves topology *for* $(26, 6)$ *pictures if all of the following conditions hold:*

1. *Only simple points can be deleted.*
2. *If a set of two, three, or four mutually 18-adjacent "1" points are deleted, then it is a simple set.*
3. *No object formed by mutually 26-adjacent points can be deleted completely.*

The three kinds of partitionings of $\mathbb{Z}^3$ into two, four, and eight subfields are illustrated in Fig. 1b-d. Without loss of generality, we can assume that $(0, 0, 0) \in SF_k(0)$ $(k = 2, 4, 8)$. We can state the following properties:

Proposition 1. *For the 4-subfield case (see Fig. 1c), two points* p *and* $q \in N_{26}(p)$ *are in the same subfield if* $q \in N_{26}(p) \setminus N_{18}(p)$.

Proposition 2. *For the 8-subfield case (see Fig. 1d), two points* p *and* $q \in N_{26}(p)$ *are* not *in the same subfield.*

As consequences of Propositions 1 and 2 if a 3D parallel reduction operation may delete some points from the subfield $SF_k(i)$ ($k = 4, 8,\ i = 0, 1, \ldots, k-1$), then we get the following simplified versions of Theorem 1:

Theorem 2. [9] *A 4-subfield 3D parallel reduction operation* preserves topology *for* $(26, 6)$ *pictures if both of the following conditions hold:*

1. *Only simple points can be deleted.*
2. *No object formed by two 26-adjacent, but not 18-adjacent points can be deleted completely.*

Theorem 3. [9] *An 8-subfield 3D parallel reduction operation* preserves topology *for* $(26, 6)$ *pictures if only simple points can be deleted.*

3 Existing Thinning Algorithms Using Four and Eight Subfields

Each existing k-subfield ($k = 4, 8$, see Fig. 1c-d) 3D thinning algorithm can be sketched by the following program:

Input: picture $(\mathbb{Z}^3, 26, 6, X)$
Output: picture $(\mathbb{Z}^3, 26, 6, Y)$

```
Y = X
repeat
    // one iteration step
    for i = 0 to k − 1 do
        // subfield SF_k(i) is activated
        D(i) = { p | p is “deletable” in Y ∩ SF_k(i) }
        Y = Y \ D(i)
until ⋃_{i=0}^{k−1} D(i) = ∅
```

Ma, Wan, and Lee [9] proposed the following two 4-subfield 3D thinning algorithms:

– **SF-4-C-MWL**: 4-subfield curve-thinning algorithm,
– **SF-4-S-MWL**: 4-subfield surface-thinning algorithm.

Deletable points of both algorithms are defined by three-color matching templates.

The three existing 8-subfield thinning algorithms proposed by Bertrand and Aktouf [1] are:

– **SF-8-C-BA**: 8-subfield curve-thinning algorithm,
– **SF-8-S-BA**: 8-subfield surface-thinning algorithm,
– **SF-8-K-BA**: 8-subfield algorithm for extracting topological kernels.

They are based on Theorem 3 (i.e., sufficient conditions for topology preservation in eight subfields) and two types of endpoint characterizations: one for surface-endpoints and one for curve-endpoints. Their algorithm for extracting topological kernels does not consider any endpoint criteria.

4 The New Subfield-Based Thinning Algorithms

We propose a set of new thinning algorithms using four and eight subfields. Their deletable points are derived directly from Theorems 2 and 3 (i.e., sufficient conditions for topology preservation for four and eight subfields, respectively). The proposed algorithms using the same kind of partitioning differ from each other just in the considered endpoint characterizations. In order to reduce the noise sensitivity and the number of skeletal points (without overshrinking the objects), we introduce a new subfield-based thinning scheme. It takes the endpoints into consideration at the beginning of iteration steps, instead of preserving them in each parallel reduction as it is accustomed in existing subfield-based thinning algorithms.

Let us consider an arbitrary characterization of endpoints that is called as type $\mathcal{E}$. Our algorithm denoted by **SF-k-$\mathcal{E}$** uses k subfields ($k = 4, 8$) and endpoints of type $\mathcal{E}$. It is outlined as follows:

Algorithm SF-k-$\mathcal{E}$.

Input: picture $(\mathbb{Z}^3, 26, 6, X)$
Output: picture $(\mathbb{Z}^3, 26, 6, Y)$

$Y = X$
repeat
  $E = \{ p \mid p$ is a border point, but not an endpoint of type $\mathcal{E}$ in $Y \}$
  for $i = 0$ **to** $k - 1$ **do**
    $D(i) = \{ q \mid q$ is an *SF-k-deletable* point in $E \cap SF_k(i) \}$
    $Y = Y \setminus D(i)$
until $\bigcup_{i=0}^{k-1} D(i) = \emptyset$

We are to lay down *SF-k-deletable* points ($k = 4, 8$):

Definition 2. *A "1" point in a* $(26, 6)$ *picture* $\mathcal{P}$ *is* self-SF-4-deletable *if it is simple in* $\mathcal{P}$ *(see Condition 1 of Theorem 2).*

Definition 3. *A "1" point* p *in a* $(26, 6)$ *picture* $\mathcal{P}$ *is* SF-4-deletable *if* p *is self-SF-4-deletable (see Definition 2), and it does not come first in the lexicographic ordering of any object* $\mathcal{O}$ *of two self-SF-4-deletable points, where* $\mathcal{O} = \{p, q\}$ *and* $q \in N_{26}(p) \setminus N_{18}(p)$ *(see Condition 2 of Theorem 2).*

It can be readily seen that simultaneous deletion of SF-4-deletable points satisfies both conditions of Theorem 2, hence it preserves the topology.

Let us define SF-8-deletable points:

Definition 4. *A "1" point in a* $(26, 6)$ *picture* $\mathcal{P}$ *is* SF-8-deletable *if it is simple in* $\mathcal{P}$.

It is easy to see that Definition 4 was derived directly from Theorem 3, hence simultaneous deletion of SF-8-deletable points is a topology preserving reduction.

We can state that all of our algorithms **SF-**k**-**$\mathcal{E}$ $(k = 4, 8)$ with any endpoint characterizations are topologically correct.

At the end of this section, we illustrate the usefulness of the new subfield-based thinning scheme (i.e., just border points in the input picture of the iteration step may be deleted). Figure 2 compares the conventional and the proposed methods using four subfields.

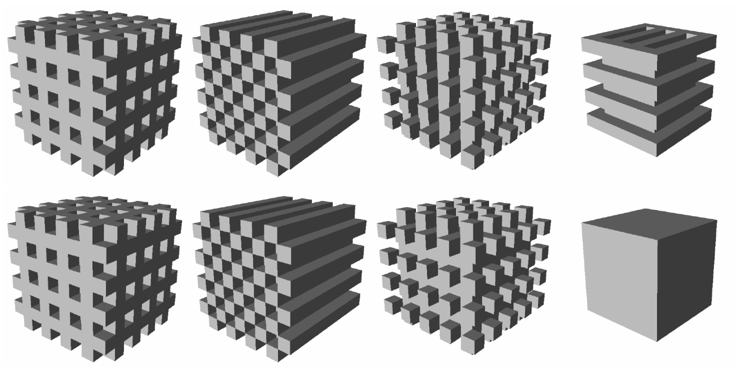

Fig. 2. One iteration step of the conventional 4-subfield thinning process (see Section 3) and the proposed thinning scheme. For simplicity, no endpoints are preserved when the $9\times9\times9$ cube is thinned. The conventional thinning may delete some points that are interior ones in the picture at the beginning of the iteration step, hence some objects may not be reduced uniformly. It may create numerous unwanted endpoints (according to some endpoint characterizations) that blocks the rest of the thinning process.

5 Examples of the Subfield-Based Thinning Algorithms

In Section 4, we defined the deletable points of the proposed algorithms that follow our new thinning scheme using iteration-level endpoint checking. Various characterizations of endpoints yield different algorithms. Here, we define six types of endpoints that determine twelve new algorithms.

Definition 5. *Any "1" point in a* $(26, 6)$ *picture is* not *an endpoint of type* **K**. *(If no endpoints are preserved, then we get topological kernels.)*

Definition 6. *A "1" point* p *in picture* $(\mathbb{Z}^3, 26, 6, B)$ *is a curve-endpoint of type* **C1** *if* $(N_{26}(p)\backslash\{p\}) \cap B = \{q\}$ *(i.e.,* p *is 26-adjacent to exactly one "1" point* q*).*

Definition 7. *A "1" point p in picture* $(\mathbb{Z}^3, 26, 6, B)$ *is a curve-endpoint of type* **C2** *if* $(N_{26}(p)\backslash\{p\}) \cap B = \{q\}$ *and*

– $(N_{26}(q)\backslash\{q\}) \cap B = \{p\}$ *or*
– $(N_{26}(q)\backslash\{q\}) \cap B = \{p, r\}$.

Note that the characterization of C2 curve-endpoints is inspired by the concept of "twig voxel" that was introduced by Ma, Wan, and Chang [8].

original (378 043) **SF-8-K-BA** (293) **SF-4-K** (288) **SF-4-K** (287)

Fig. 3. A 304 × 96 × 261 image of a helicopter and its topological kernels produced by the three algorithms under comparison. The original image contains just one object, there is no cavity in it, and the skid of the helicopter consists of two holes that are preserved in the topological kernels (i.e., minimal structures which are topologically equivalent to the original helicopter).

Definition 8. *A "1" point p in picture* $(\mathbb{Z}^3, 26, 6, B)$ *is a surface-endpoint of type* **S1** *if there is no interior point in the set* $N_6(p) \cap B$.

Definition 9. *A "1" point p in picture* $(\mathbb{Z}^3, 26, 6, B)$ *is a surface-endpoint of type* **S2** *if there is no interior point in the set* $N_{18}(p) \cap B$.

Definition 10. *A "1" point p in picture* $(\mathbb{Z}^3, 26, 6, B)$ *is a surface-endpoint of type* **S3** *if there is no interior point in the set* $N_{26}(p) \cap B$.

Note that these three characterizations of surface-endpoints are hidden in the algorithms proposed by Manzanera et al. [10].

In experiments our twelve new algorithms based on four and eight subfields and using the endpoints according to Definitions 5-10 were tested on objects of different shapes. Here we present some illustrative examples below (Figures 3-7). Numbers in parentheses mean the count of "1" points. Skeleton-like shape features produced by the proposed twelve algorithms are compared with the results of 8-subfield algorithms **SF-8-K-BA**, **SF-8-C-BA**, and **SF-8-S-BA** proposed by Bertrand and Aktouf [1]. Unfortunately, we could not make credible implementations of the two existing 4-subfield algorithms **SF-4-C-MWL** and **SF-4-S-MWL** proposed by Ma, Wan, and Lee [9].

Note that our algorithms are not time consuming and it is easy to implement them on conventional sequential computers by adapting the efficient implementation method presented in [13]. Skeleton-like features can be extracted from large 3D shapes within one second by the proposed algorithms on a usual PC.

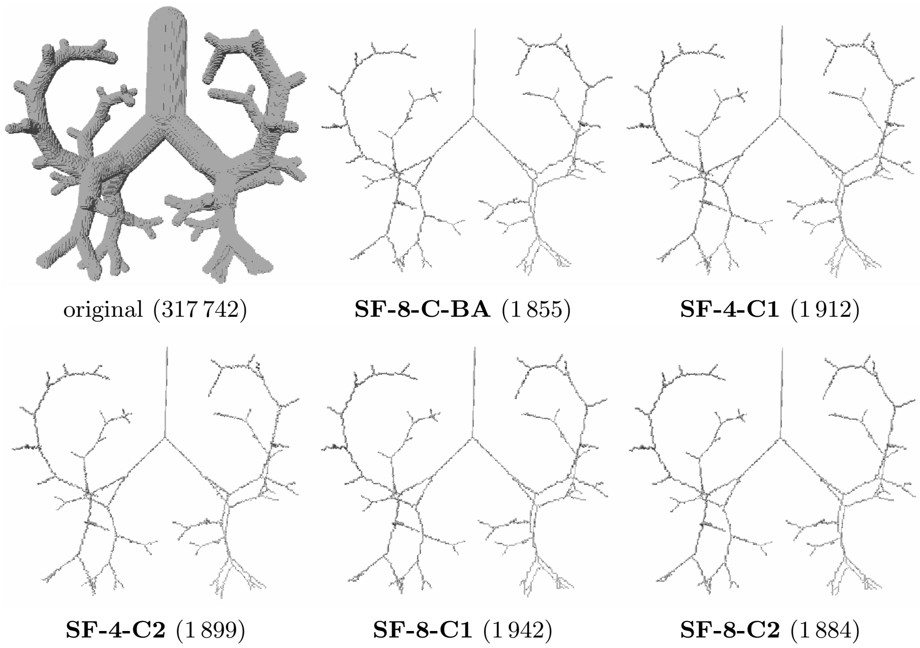

Fig. 4. A $300 \times 300 \times 300$ image of a tubular structure and its centerlines produced by the five algorithms under comparison

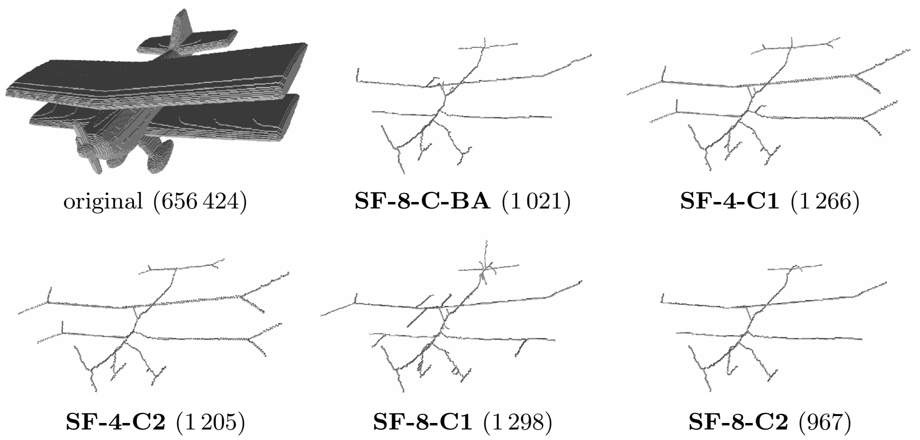

Fig. 5. A $217 \times 304 \times 98$ image of an airplane and its centerlines produced by the five algorithms under comparison

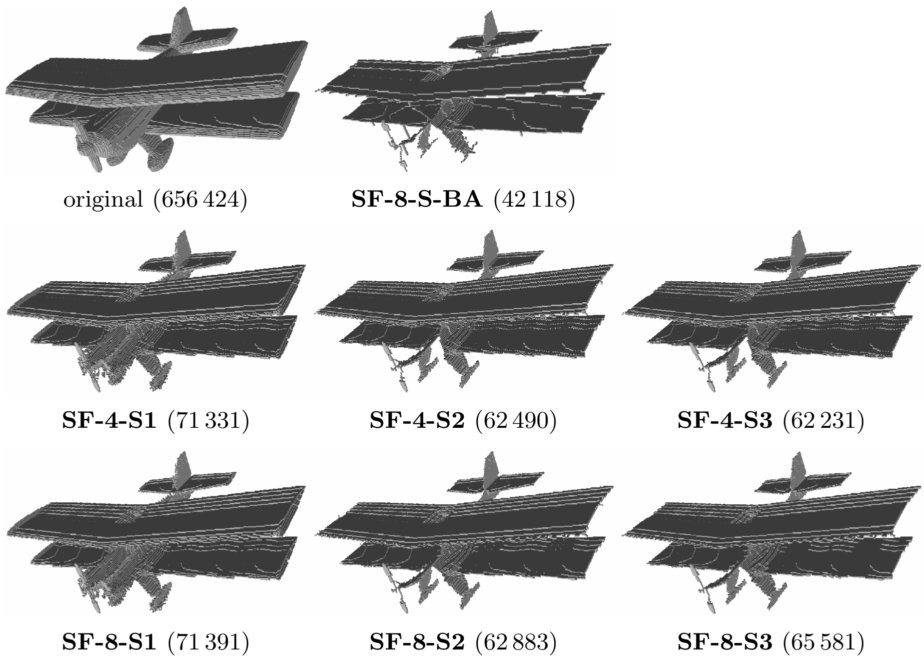

Fig. 6. A $217 \times 304 \times 98$ image of an airplane and its medial surfaces produced by the seven algorithms under comparison

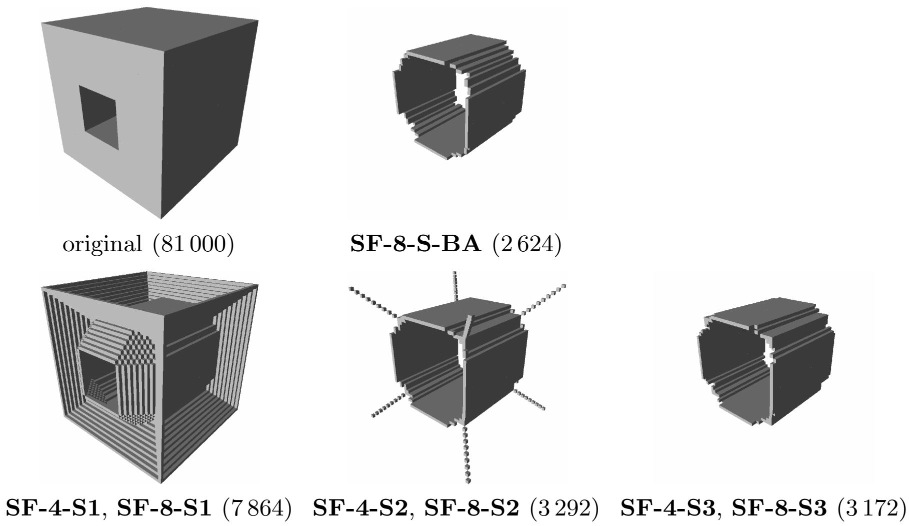

Fig. 7. The 3D image of a $45 \times 45 \times 45$ cube with a hole and its medial surfaces produced by the seven algorithms under comparison. Interestingly, the same medial surfaces are extracted from this special object by the corresponding 4-subfield and 8-subfield algorithms

Acknowledgements. This research was supported by the TÁMOP-4.2.2/08/1/2008-0008 program of the Hungarian National Development Agency, the NKTH-OTKA-CNK80370 Grant, and the National Office for Research and Technology.

References

1. Bertrand, G., Aktouf, Z.: A 3D thinning algorithm using subfields. In: SPIE Proc. of Conf. on Vision Geometry, pp. 113–124 (1994)
2. Gomberg, B.R., Saha, P.K., Song, H.K., Hwang, S.N., Wehrli, F.W.: Topological analysis of trabecular bone MR images. IEEE Transactions on Medical Imaging 19, 166–174 (2000)
3. Hall, R.W.: Parallel connectivity-preserving thinning algorithms. In: Kong, T.Y., Rosenfeld, A. (eds.) Topological algorithms for digital image processing, pp. 145–179. Elsevier Science, Amsterdam (1996)
4. Itoh, T., Yamaguchi, Y., Koyamada, K.: Fast isosurface generation using the volume thinning algorithm. IEEE Transactions on Visualization and Computer Graphics 7, 32–46 (2001)
5. Kong, T.Y., Rosenfeld, A.: Digital topology: Introduction and survey. Computer Vision, Graphics, and Image Processing 48, 357–393 (1989)
6. Ma, C.M.: On topology preservation in 3D thinning. CVGIP: Image Understanding 59, 328–339 (1994)
7. Ma, C.M., Wan, S.Y.: A medial-surface oriented 3-d two-subfield thinning algorithm. Pattern Recognition Letters 22, 1439–1446 (2001)
8. Ma, C.M., Wan, S.Y., Chang, H.K.: Extracting medial curves on 3D images. Pattern Recognition Letters 23, 895–904 (2002)
9. Ma, C.M., Wan, S.Y., Lee, J.D.: Three-dimensional topology preserving reduction on the 4-subfields. IEEE Transaction on Pattern Analysis and Machine Intelligence 24, 1594–1605 (2002)
10. Manzanera, A., Bernard, T.M., Prêteux, F., Longuet, B.: Medial faces from a concuise 3D thinning algorithm. In: Proc. 7th IEEE Int. Conf. on Computer Vision, pp. 337–343 (1999)
11. Németh, G., Kardos, P., Palágyi, K.: Topology preserving 2-subfield 3D thinning algorithms. In: Proc. 7th IASTED Int. Conf. Signal Processing, Pattern Recognition and Applications, pp. 310–316 (2009)
12. Palágyi, K., Tschirren, J., Hoffman, E.A., Sonka, M.: Quantitative analysis of pulmonary airway tree structures. Computers in Biology and Medicine 36, 974–996 (2006)
13. Palágyi, K., Németh, G.: Fully parallel 3D thinning algorithms based on sufficient conditions for topology preservation. In: Brlek, S., Reutenauer, C., Provençal, X. (eds.) DGCI 2009. LNCS, vol. 5810, pp. 481–492. Springer, Heidelberg (2009)
14. Shaked, D., Bruckstein, A.: Pruning medial axes. Computer Vision and Image Understanding 69, 156–169 (1998)
15. Sundar, H., Silver, D., Gagvani, N., Dickinson, S.: Skeleton based shape matching and retrieval. In: Proc. Int. Conf. Shape Modeling and Applications, pp. 130–139 (2003)
16. Wan, M., Liang, Z., Ke, Q., Hong, L., Bitter, I., Kaufman, A.: Automatic centerline extraction for virtual colonoscopy. IEEE Transactions on Medical Imaging 21, 1450–1460 (2002)